Vanadium(V) Complexes of 2,2′-Thiobis(4-methyl-6-*tert*-butylphenol) (H_2mbp_2S) and 2,2′-Sulfinylbis(4-methyl-6-*tert*-butylphenol) (H_2mbp_2SO)

Charles R. Cornman,*,† Katherine M. Geiser-Bush,† and Jeff W. Kampf‡

Department of Chemistry, North Carolina State University, Raleigh, North Carolina 27695-8204, and Department of Chemistry, University of Michigan, Ann Arbor, Michigan 48109-1055

Received January 6, 1999

The sulfide-containing ligand 2,2′-thiobis(4-methyl-6-*tert*-butylphenol), H_2mbp_2S, coordinates facially to vanadium forming six-coordinate alkoxide- (**1**) or hydroxide-bridged (**2**) dimers that have been structurally characterized. ^{51}V NMR indicates that structural isomers are present. Electrochemical studies indicate that the metal centers in **1** are strongly coupled ($K_{com} \approx 10^5$). The corresponding sulfoxide, H_2mbp_2SO, coordinates to vanadium(V) to form a six-coordinate complex with a 2:1 L:M stoichiometry. Under the conditions of this study, direct oxygenation of the coordinated sulfide in **1** and **2** has not been observed. Crystal data for **1** ($C_{55}H_{74}O_8S_2V_2$): space group *R*-3, $a = 35.6184(2)$ Å, $b = 35.6184(2)$ Å, $c = 13.52170(10)$ Å, $\alpha, \beta = 90°$, $\gamma = 120°$, $Z = 18$. Crystal data for **2** ($C_{26}H_{35}N_2O_4SV$): space group *P*2(1)/*n*, $a = 13.2894(2)$ Å, $b = 12.9652(2)$ Å, $c = 16.3639(2)$ Å, $\alpha,\gamma = 90°$, $\beta = 102.43°$, $Z = 4$. Crystal data for **3** ($C_{50}H_{70}O_7S_2V$): space group *P*-1, $a = 9.1567(5)$ Å, $b = 13.9314(8)$ Å, $c = 19.7196(11)$ Å, $\alpha = 79.1460(10)°$, $\beta = 86.5840(10)°$, $\gamma = 82.7570(10)°$, $Z = 2$.

Introduction

Metal-catalyzed reactions of organosulfur compounds are of biological and industrial importance.[1] Recently, catalytic oxygenation of organosulfur compounds has found increased application in asymmetric synthesis.[2] Kagan has reported the oxidation of sulfides to sulfoxides using a modification of the Sharpless epoxidation reaction, which uses titanium tartrates as the chiral catalysts.[3] Several workers have shown that under general conditions $VO(acac)_2$ in association with a chiral Schiff base ligand is an effective catalyst for the asymmetric oxygenation of prochiral sulfides.[4−6] Vanadium proteins, such as the vanadium adduct of phytase and vanadium haloperoxidases, can also catalyze the asymmetric oxidation of sulfides.[7,8] In both the titanium and vanadium systems, peroxide is activated by coordination to the high-valent metal center.

Vanadium(V)−sulfur interactions are also important in a biological context since the vanadium−thiol structural unit is believed responsible for the potent reversible inhibition of protein tyrosine phosphatases (PTPs), enzymes that regulate phosphate-based intracellular signal transduction.[9−12] Protein crystallography of three vanadium−PTP adducts confirms that the five-coordinate vanadium has a trigonal bipyramidal geometry in which the oxo ligand is equatorial and the thiolate sulfur is axial.[13−15] It has also been shown that peroxovanadium complexes can oxidize the active site cysteine of PTPs, thereby causing irreversible inhibition.[16]

Despite this research activity, well-characterized oxovanadium(V) complexes containing organosulfur ligands are rare.[17−19] This is due, at least in part, to the tendency of vanadium(V) to oxidize low-valent sulfur. We have reported the synthesis and structure of two oxovanadium(V)−thiolate complexes, in which the thiolate ligand is one arm of a tripodal, tetradentate ligand.[18,19] The coordinated thiolate can be quantitatively oxygenated with peroxides to form the corresponding oxovanadium−η^2-sulfenate complexes as shown in eq 1a. In this

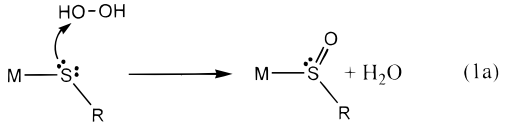

(1a)

reaction, it is likely that direct electrophilic attack of the peroxide

† North Carolina State University.
‡ University of Michigan.

(1) Stiefel, E. I. *Transition Metal Sulfur Chemistry: Biological and Industrial Significance and Key Trends*; Stiefel, E. I., Ed.; American Chemical Society: Washington, DC, 1996; pp 2−38.
(2) Cogan, D. A.; Liu, G.; Kim, K.; Backes, B. J.; Ellman, J. A. *J. Am. Chem. Soc.* **1998**, *120*, 8011−8019.
(3) Kagan, H. B.; Rebiere, F.; Samuel, O. *Phosphorus, Sulfur Silicon Relat. Elem.* **1991**, *58*, 89−110.
(4) Bolm, C.; Bienewald, F. *Angew. Chem., Int. Ed. Engl.* **1995**, *34*, 2640−2642.
(5) Nakajima, K.; Kojima, K.; Kojima, M.; Fujita, J. *Bull. Chem. Soc. Jpn.* **1990**, *63*, 2620.
(6) Nakajima, K.; Kojima, M.; Toriumi, K.; Saito, K.; Fujita, J. *Bull. Chem. Soc. Jpn.* **1989**, *62*, 760.
(7) ten Brink, H. B.; Tuynman, A.; Dekker, H. L.; Hemrika, W.; Izumi, Y.; Oshiro, T.; Schoemaker, H. E.; Wever, R. *Inorg. Chem.* **1998**, *37*, 6780−6784.
(8) Andersson, M.; Willetts, A.; Allenmark, S. *J. Org. Chem.* **1997**, *62*, 8455−8458.
(9) Zhang, Z.-Y.; Dixon, J. E. *Adv. Enzymol. Relat. Areas Mol. Biol.* **1994**, *68*, 1−36.
(10) Pot, D. A.; Dixon, J. E. *Biochim. Biophys. Acta* **1992**, *1136*.
(11) Fischer, E. H.; Charboneau, H.; Tonks, N. K. *Science* **1991**, *253*, 401−406.
(12) Tonks, N. K.; Flint, A. J.; Gebbink, M. F. B. G.; Sun, H.; Yang, Q. *Adv. Second Messeng. Phosphoprot. Res.* **1993**, *28*, 203−210.
(13) Zhang, M.; Zhou, M.; Van Etten, R. L.; Stauffacher, C. V. *Biochemistry* **1997**, *36*, 15−23.
(14) Denu, J. M.; Lohse, D. L.; Vijayalakshmi, J.; Saper, M.; Dixon, J. E. *Proc. Natl. Acad. Sci. U.S.A.* **1996**, *93*, 2493−2498.
(15) Pannifer, A. D. B.; Flint, A. J.; Tonks, N. K.; Barford, D. *J. Biol. Chem.* **1998**, *273*, 10454−10462.
(16) Huyer, G.; Liu, S.; Kelly, J.; Moffat, J.; Payette, P.; Kennedy, B.; Tsaprailis, G.; Gresser, M. J.; Ramachandran, C. *J. Biol. Chem.* **1997**, *272*, 843.
(17) Sendlinger, S. C.; Nicholson, J. R.; Lobkovsky, E. B.; Huffman, J. C.; Rehder, D.; Christou, G. *Inorg. Chem.* **1993**, *32*, 204−210.
(18) Cornman, C. R.; Stauffer, T. C.; Boyle, P. D. *J. Am. Chem. Soc.* **1997**, *119*, 5986−5987.

10.1021/ic9900253 CCC: $18.00
Published on Web 09/01/1999

on the coordinated thiol is responsible for the oxygen atom transfer. A similar mechanism has been proposed for the oxygenation of nickel−thiolates to nickel−η^1-sulfenates;[20,21] however, it should be noted that vanadium−peroxide coordination has not been ruled out by kinetic studies. Rehder and co-workers have examined the vanadium-catalyzed oxygenation of sulfides to sulfoxides and sulfones (eq 1b).[22] Spectroscopic studies of the

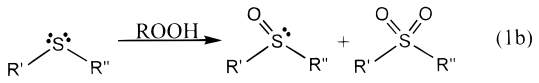

(1b)

catalytic vanadium Schiff base complexes in the presence of excess sulfide or sulfoxide have indicated interactions between the vanadium complex and both the sulfide (weak) and sulfoxide (stronger). In this contribution, we report the synthesis, structure, and reactivity of vanadium complexes of sulfides and sulfoxides in which the S/SO groups are the central donor of the tridentate ligands 2,2′-thiobis(4-methyl-6-*tert*-butylphenol) (H_2mbp_2S) and its oxygenation product 2,2′-sulfinylbis(4-methyl-6-*tert*-butylphenol) (H_2mbp_2SO, eq 2).

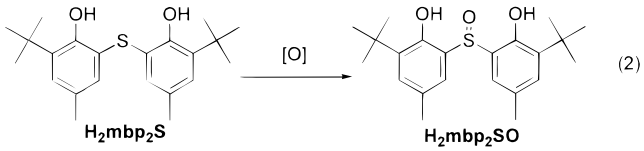

(2)

Experimental Procedures

All chemicals were used as received from commercial sources unless otherwise noted. Toluene was distilled from sodium. The H_2mbp_2S ligand was prepared following the procedures of Prakasha and co-workers.[23] The H_2mbp_2SO ligand was prepared following the procedures of Okuda and co-workers.[24]

[VO(mbp$_2$S)(OEt)]$_2$·1.2tol (1). The H_2mbp_2S ligand (0.400 g, 1.12 mmol) was dissolved in 10 mL of dry, distilled toluene under N_2. VO(O-*i*-Pr)$_3$ (0.263 mL, 1.12 mmol) was added, and the mixture was stirred at room temperature for 30 min. The reaction mixture turned dark purple immediately upon addition of VO(O-*i*-Pr)$_3$. The mixture was exposed to air, layered with 10 mL of absolute ethanol, and allowed to sit. After approximately 18 h, dark purple crystalline needles, suitable for X-ray crystallography, were filtered from the solution. Crystals lose solvent and easily splinter upon removal from the mother liquor. Yield 0.393 g, 75%. ν(V=O) 985 cm^{-1}. Calculated for [VO(mbp$_2$S)(OEt)]$_2$·1.2tol, $C_{74.4}H_{75.6}O_8S_2V_2$ (Found): %C, 64.52 (64.66); %H, 7.24 (7.27); %S, 6.24 (6.12); %V, 9.61 (9.72). UV−vis spectrum (CH_2Cl_2, energy/10^3 cm^{-1} (ϵ/10^3 M^{-1}cm^{-1})): 12.5 (5.1), 19.4 (10.0), 20.8 (sh).

[VO(mbp$_2$S)(OH)]$_2$·2CH$_3$CN (2). The H_2mbp_2S ligand (0.302 g, 0.842 mmol) was dissolved in 10 mL of reagent grade acetonitrile in air. VO(O-*i*-Pr)$_3$ (0.199 mL, 0.842 mmol) was added, and the mixture was stirred at room temperature for 90 min. The reaction mixture turned dark purple immediately upon addition of VO(O-*i*-Pr)$_3$, and after about 10 min of stirring a dark purple microcrystalline solid began to precipitate from solution. The hydroxide ligands in **2** are presumably derived from aerobic moisture or residual moisture in the solvent (≤0.3% water in Aldrich reagent grade CH_3CN). The crystals were filtered from the solution and rinsed with water. Crystals suitable for X-ray crystallography were grown over 48 h from a dilute and unstirred acetonitrile solution. Yield: 0.375 g, 92%. ν(V=O) 995 cm^{-1}. Calculated for [VO(mbp$_2$S)(OH)]$_2$·2.5H$_2$O, $C_{44}H_{63}O_{10.5}S_2V_2$ (Found): %C, 57.07 (57.13); %H, 6.86 (6.47); %N, 0.00 (0.40); %S, 6.92 (6.97). UV−vis spectrum (CH_2Cl_2, energy/10^3 cm^{-1} (ϵ/10^3 M^{-1}cm^{-1})): 12.7 (6.5), 19.6 (12.3), 21.7 (sh).

VO(mbp$_2$SO)(Hmbp$_2$SO) (3). The H_2mbp_2SO ligand (0.302 g, 0.806 mmol) was stirred with VO(O-*i*-Pr)$_3$ (0.190 mL, 0.806 mmol) in about 10 mL of absolute ethanol. The stirring was stopped after a few minutes and the solution allowed to sit undisturbed. After 24 h dark purple crystals were filtered from the solution and washed with 2 × 1 mL of H_2O and a small amount of cold ethanol. The crystals were dried by vacuum aspiration. Yield: 0.184 g. X-ray quality crystals were grown from a hexane solution. Calculated for VO(mbp$_2$SO)(Hmbp$_2$SO), $C_{44}H_{57}O_7S_2V$ (Found): %C, 65.00 (65.04); %H, 7.07 (7.16); %S, 7.89 (7.89). UV−vis spectrum (CH_2Cl_2, energy/10^3 cm^{-1} (ϵ/10^3 M^{-1}cm^{-1})): 19.1 (7.7), 24.8 (5.1).

X-ray Crystal Structure Analysis. Crystallographic data and details of the data acquisition for complexes **1**−**3** are shown in Table 1. Structural determinations were performed using a Siemens SMART CCD-based X-ray diffractometer equipped with a normal focus Mo-target X-ray tube (λ = 0.71073 Å) operated at 2000 W power (50 kV, 40 mA). X-ray intensities were measured at 158 K and the frames integrated with the Siemens SAINT software package with a narrow frame algorithm. Analysis of the data showed negligible decay during data collection. Final *R*-values based on refinement on F^2 are provided in Table 1. Selected bond distances and angles are provided in Tables 2 and 3.

For complex **1**, a full sphere of data consisting of a total of 2132 frames was collected with a scan width of 0.3° in ω and an exposure time of 60 s/frame. The integration of the data using a trigonal unit cell yielded a total of 103 904 reflections to a maximum 2θ value of 49.7° of which 16 849 were independent. Due to the paucity of high-angle data, reflections of $2\theta > 45°$ were excluded from the refinement. The final cell constants (Table 1) were based on the *xyz* centroids of 8192 reflections above $10\sigma(I)$. The structure was solved and refined using the space group *R*-3 with $Z = 9$ for the formula $C_{55}H_{74}O_8S_2V_2$, which includes 0.5 molecule of toluene solvate per asymmetric unit. All non-hydrogen atoms were refined anisotropically with the hydrogen atoms placed in idealized positions.

For **2**, a full sphere of data consisting of a total of 2132 frames was collected with a scan width of 0.3° in ω and an exposure time of 60 s/frame. The integration of the data using a primitive monoclinic unit cell yielded a total of 27 979 reflections to a maximum 2θ value of 56.7° of which 7006 were independent. The final cell constants (Table 1) were based on the *xyz* centroids of 6940 reflections above $10\sigma(I)$. The data were corrected for absorption using an empirical correction. The structure was solved and refined using the space group $P2(1)/n$ with $Z = 4$ for the formula $C_{26}H_{35}N_2O_4SV$, which includes two molecules of acetonitrile solvate per asymmetric unit. All non-hydrogen atoms were refined anisotropically with the hydrogen atoms located on a difference map and allowed to refine isotropically.

For complex **3**, a full sphere of data consisting of a total of 2132 frames was collected with a scan width of 0.3° in ω and an exposure time of 75 s/frame. The integration of the data using a triclinic unit cell yielded a total of 25 069 reflections to a maximum 2θ value of 53.7° of which 9891 were independent. The final cell constants (Table 1) were based on the *xyz* centroids of 5058 reflections above $10\sigma(I)$. The data were not corrected for absorption. The structure was solved and refined using the space group *P*-1 with $Z = 2$ for the formula $C_{50}H_{70}O_7S_2V_2$, which includes a hexane solvate molecule. All non-hydrogen atoms were refined anisotropically with the exception of the solvate. Hydrogen atoms were placed in idealized positions except for the assumed hydrogen on O6 (based on charge balance), which was not used in this model.

Spectroscopy. Infrared spectra were obtained on KBr pellets using a Bio-Rad FTS 6000 spectrometer. Electrochemical data was obtained

(19) Cornman, C. R.; Stauffer, T. C.; Boyle, P. D. *Synthesis, Structure, and Reactivity of V^V-Thiolate and V^V-η^2-Sulfenate Complexes*; Tracey, A. S., Crans, D. C., Eds.; American Chemical Society: Washington, DC, 1998; pp 71−81.
(20) Grapperhaus, C. A.; Darensbourg, M. Y. *Acc. Chem. Res.* **1998**, *31*, 451−459.
(21) Maroney, M. J.; Choudhury, S. B.; Sherrod, M. J. *Inorg. Chem.* **1996**, *35*, 1073−1076.
(22) Schmidt, H.; Bashirpoor, M.; Rehder, D. *J. Chem. Soc., Dalton Trans.* **1996**, 3865−3870.
(23) Prakasha, T. K.; Day, R. O.; Holmes, R. R. *J. Am. Chem. Soc.* **1993**, *115*, 2690−2695.
(24) Okuda, J.; Fokken, S.; Kang, H.-C.; Massa, W. *Polyhedron* **1998**, *17*, 943−946.

Table 1. Crystallographic Data for Complexes **1**−**3**

	1	**2**	**3**
empirical formula	$C_{55}H_{74}O_8S_2V_2$	$C_{26}H_{35}N_2O_4SV$	$C_{50}H_{70}O_7S_2V$
formula weight (calcd)	514.57	552.56	898.12
temperature (K)	158 (2)	158 (2)	158 (2)
wavelength (Å)	0.71073	0.71073	0.71073
crystal system	trigonal	monoclinic	triclinic
space group	*R*-3	*P*2(1)/*n*	*P*-1
a (Å)	35.6184 (2)	13.2894 (2)	9.1567 (5)
b (Å)	35.6184 (2)	12.9652 (2)	13.9314 (8)
c (Å)	13.52170 (10)	16.3639 (2)	19.7196 (11)
α (deg)	90	90	79.1460 (10)
β (deg)	90	102.4300 (10)	86.5840 (10)
γ (deg)	120	90	82.7570 (10)
volume (Å^3)	14856.3 (2)	2753.41 (7)	2449.2 (2)
Z	18	4	2
density (calcd, mg/m^3)	1.035	1.261	1.218
absorption coeff (mm^{-1})	0.388	0.468	0.336
R1 [$I > 2\sigma(I)$]	0.0996	0.0536	0.1448
wR2 [$I > 2\sigma(I)$]	0.2359	0.0996	0.3081

[a] $R1 = \sum||F_o| - |F_c||/\sum|F_o|$. [b] $wR2 = (\sum[w(F_o^2 - F_c^2)^2]/\sum[wF_o^4])^{1/2}$.

Table 2. Selected Bond Lengths (Å) and Angles (deg) for Complexes **1** and **2**

	1	**2**
V−O1	1.588(6)	1.593(2)
V−O2	1.985(5)	1.973(2)
V−O2a	1.974(5)	1.973(2)
V−O3	1.828(6)	1.838(2)
V−O4	1.845(6)	1.861(2)
V−S	2.797(2)	2.7953(7)
O1−V−O2	102.7(3)	101.85(8)
O1−V−O2a	102.6(3)	103.76(8)
O1−V−O3	100.0(3)	97.89(8)
O1−V−O4	98.4(3)	99.79(8)
O1−V−S	173.8(2)	172.33(7)
O2−V−O2a	72.5(2)	73.49(8)
O2−V−O3	91.0(2)	157.27(7)
O2−V−O4	156.6(2)	91.39(7)
O2−V−S	82.7(2)	84.96(5)
O2a−V−O3	154.4(2)	91.01(7)
O2a−V−O4	93.3(2)	154.12(7)
O2a−V−S	81.9(2)	81.43(5)
O3−V−O4	95.2(2)	96.28(7)
O3−V−S	76.6(2)	76.18(5)
O4−V−S	76.9(2)	76.31(5)
V−O2−Va	107.5(2)	106.50(8)

Table 3. Selected Bond Lengths (Å) and Angles (deg) for Complex **3**

V−O1	1.569(7)
V−O2	1.849(7)
V−O3	1.862(7)
V−O4	2.229(7)
V−O5	1.888(7)
V−O7	2.050(7)
O1−V−O2	97.9(3)
O1−V−O3	99.8(3)
O1−V−O4	174.8(3)
O1−V−O5	93.5(3)
O1−V−O7	98.1(3)
O2−V−O3	92.7(3)
O2−V−O4	84.4(3)
O2−V−O5	96.7(3)
O2−V−O7	163.8(3)
O3−V−O4	84.8(3)
O3−V−O5	162.6(3)
O3−V−O7	81.9(3)
O4−V−O5	81.6(3)
O4−V−O7	79.9(3)
O5−V−O7	85.0(3)

using an EG&G Model 273 electrochemical system. Cyclic voltammograms were obtained on CH_2Cl_2 solutions with 0.1 M $TBAPF_6$ as supporting electrolyte, using a standard three-electrode configuration with a nonaqueous Ag(s)/$AgNO_3$ reference electrode (0.01 M $AgNO_3$ in 0.1 M $TBAPF_6$ in CH_3CN) and a glassy carbon working electrode. Under these conditions, the reversible ferrocene/ferrocinium couple occurred at 0.222 ± 0.001 V ($\Delta E = 80-91$ mV; $i_c/i_a \approx 1$). Vanadium-51 NMR spectra were obtained on a GE Omega 300 instrument operating at 79 MHz and ambient temperature (20−25 °C). External V^VOCl_3 ($\delta = 0$ ppm) was used as reference. Errors in the observed chemical shift are estimated to be ±0.3 ppm. UV−vis spectra were obtained from ca. 0.05 mM solutions in CH_2Cl_2 using a Hewlett-Packard 8452A diode array spectrophotometer.

Results and Discussion

Syntheses and Structures. The structures of several transition metal complexes of H_2mbp_2S (or similar ligands) have been reported. Complexes of Ti(IV),[25,26] W(VI),[27] and Co(II)[28,29] have distorted octahedral geometries, while Cu(II) can form octahedral[30] or square planar[31] complexes. In all cases, the $[mbp_2S]^{2-}$ dianion coordinates using both phenolate oxygen donors and the sulfide sulfur donor. The $[mbp_2S]^{2-}$ ligand also forms complexes with phosphorus(V) yielding trigonal bipyramidal structures.[32]

Reaction of an equivalent of the H_2mbp_2S ligand with an equivalent of $V^VO(O\text{-}i\text{-}Pr)_3$ in toluene immediately yields a deep purple solution. Addition of ethanol yields a purple precipitate that has been assigned the ethoxide-bridged dimeric structure $[VO(mbp_2S)OEt]_2$, **1**, based on elemental analysis and X-ray crystallography. If the reaction is carried out in CH_3CN and ethanol is excluded, the corresponding hydroxide-bridged

(25) Fokken, S.; Spaniol, T. P.; Kang, H.-C.; Massa, W.; Okuda, J. *Organometallics* **1996**, *15*, 5069−5072.
(26) Porri, L.; Ripa, A.; Colombo, P.; Miano, E.; Capelli, S.; Meille, S. V. *J. Organomet. Chem.* **1996**, *514*, 213−217.
(27) Berges, V. P.; Hinrichs, W.; Holzmann, A.; Wiese, J.; Klar, G. *J. Chem. Res. (M)* **1986**, 201−215.
(28) Berges, V. P.; Hinrichs, W.; Holzmann, A.; Wiese, J.; Klar, G. *J. Chem. Res.* **1986**, 245−263.
(29) Muller, H.; Holzmann, A.; Hinrichs, W.; Klar, G. *Z. Naturforsch.* **1982**, *37b*, 341−347.
(30) Holzmann, A.; Berges, P.; Hinrichs, W.; Klar, G. *J. Chem. Res. (S)* **1987**, 42−43.
(31) Chaudhouri, P.; Hess, M.; Flörke, U.; Wieghardt, K. *Angew. Chem., Int. Ed.* **1998**, *37*, 2217−2220.
(32) Sherlock, D. J.; Chandrasekaran, A.; Day, R. O.; Holmes, R. R. *Inorg. Chem.* **1997**, *36*, 5082−5089.

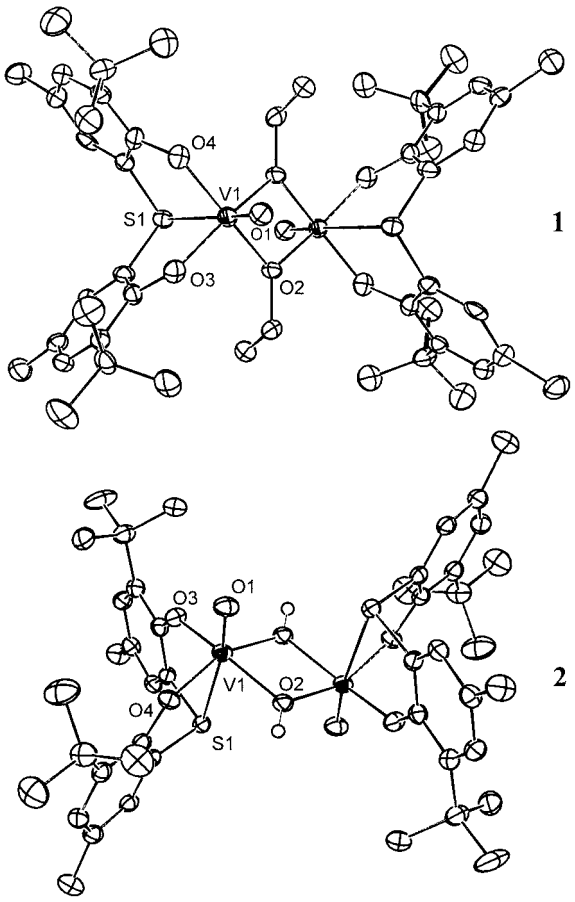

Figure 1. Molecular structures of **1** (top) and **2** (bottom). Thermal ellipsoids are at 50% probability.

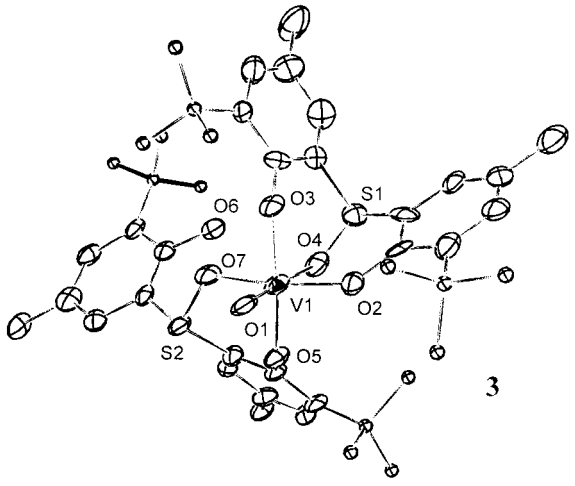

Figure 2. Molecular structure of **3**. Thermal ellipsoids are at 50% probability except for the *tert*-butyl carbons which are spheres of arbitrary size (for clarity).

structure, **2**, is formed. The hydroxide ligands are presumably derived from air or residual water in the solvent. When the corresponding sulfoxide ligand H_2mbp_2SO is used, the deep purple mononuclear complex $VO(mbp_2SO)(Hmbp_2SO)$ is isolated in which one of the phenol groups is protonated and pendant.

The X-ray structures of **1** and **2** are shown in Figure 1 and the structure of **3** is shown in Figure 2. Important bond distances and angles are presented in Tables 2 and 3. Complexes **1** (Figure 1, top) and **2** (Figure 1, bottom) are composed of two edge-shared octahedra in which the $[mbp_2S]^{2-}$ ligand coordinates facially with the sulfur donor positioned trans to the oxo donor atom. Two ethoxide groups bridge the vanadium atoms in **1**, while two hydroxide ligands bridge the vanadium atoms in **2**. The V−V distance in the ethoxide-bridged complex **1** (3.19 Å) is nearly the same as the corresponding distance in the hydroxide-bridged complex **2** (3.16 Å). The bridge in **1** is asymmetric with V−O(2) at 1.985(5) Å and V−O(2A) at 1.974(5) Å. In **2**, the bridge is symmetric with V−O(2) at 1.973(2) Å. The axial V−S distance is 2.797(2) Å and 2.7953(7) Å in **1** and **2**, respectively. This is significantly longer than the equatorial V−S in oxovanadium(V)−thiolate complexes (≈2.25 Å)[18,19,33] as one would expect based on a structural trans influence for the S donor trans to the oxo ligand. One would further expect the neutral diaryl sulfide sulfur to be a weaker donor than anionic thiolate sulfur; however, direct comparison between equatorial and axial sulfides could not be made due to the absence of appropriate, structurally characterized complexes. The mean displacements from the equatorial planes are 0.34 and 0.33 Å in **1** and **2**, respectively.

The mononuclear sulfoxide complex **3** is best described as a distorted octahedron with two mbp_2SO ligands per oxovanadium(V). This structure is similar to that proposed (but not fully characterized) for a titanium(IV) complex of this ligand.[34] In **3**, the first $[mbp_2SO]^{2-}$ ligand coordinates facially in the manner seen for **1** and **2** *except* that the axial donor is a sulfoxide oxygen, not a sulfide sulfur. The second ligand occupies the remaining two equatorial coordination sites using phenolate oxygen and sulfoxide oxygen. The second phenol of the mbp_2SO ligand is uncoordinated, and it is assumed that it remains protonated. The vanadium−phenolate oxygen bond distances for the facially coordinated ligand in **3** (V−O(2) 1.849(7) Å, V−O(3) 1.862(7) Å) are similar to those in **1** (V−O(3) 1.828(6) Å, V−O(4) 1.845(6) Å) and **2** (V−O(3) 1.838(2) Å, V−O(4) 1.861(2) Å). The vanadium−phenolate oxygen bond distance in the second, bidentate ligand in **3** is longer with V−O(5) at 1.888(7) Å. These distances (average = 1.856 Å) are shorter than the mean for currently characterized oxovanadium−phenolate oxygen bonds (1.912 Å), but still within the range of V−O(phenoxide) bond distances (1.735−2.460 Å).[35]

The vanadium-to-axial sulfoxide oxygen (V−O4) distance is 2.229(7) Å, which is considerably shorter than the corresponding V−S distances in **1** and **2**, consistent with the expectation that the sulfoxide oxygen is a better ligand than sulfide sulfur for oxovanadium(V). The vanadium-to-equatorial sulfoxide oxygen (V−O7) distance is 2.050(7) Å, which is ≈0.1 Å longer than the $V-O_{bridge}$ distances in **1** and **2**. To the best of our knowledge, this is the only example of this structural motif. It is interesting to note that the VL_2 complex is the only isolated material, even under conditions that should favor dimer formation as seen for **1** and **2**. This suggests that the bidentate sulfoxide−phenolate fragment of $[Hmbp_2SO]^{1-}$ is stable relative to the potential alkoxide-bridged dimeric structure. It is noted that the sulfoxide ligand forms six-membered chelates whereas the sulfide ligand of **1** and **2** forms five-membered chelates.

The purple color of these complexes (see Experimental Section) is presumably due to the phenolate-to-metal charge transfer as is seen for other oxovanadium (V) complexes of phenolate-derived ligands. The absence in **3** of the low-energy

(33) Nanda, K. K.; Sinn, E.; Addison, A. W. *Inorg. Chem.* **1996**, *35*, 1−2.
(34) Okuda, J.; Fokken, S.; Kang, H.-C.; Massa, W. *Polyhedron* **1998**, *17*, 943−946.
(35) Allen, F. H.; Kennard, O. *Chem. Des. Autom. News* **1993**, *8*, 31−37.

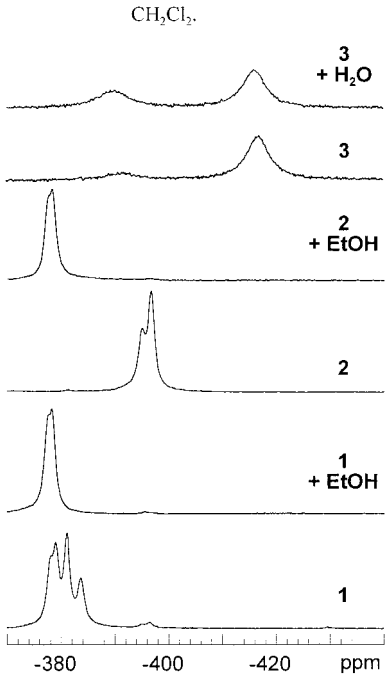

Figure 3. ^{51}V NMR spectra of **1**−**3**. Conditions: ambient temperature (20−25 °C), ca. 1 mM, in CH_2Cl_2.

transition (>800 nm) suggests that this transition may be indicative of the trans OV ← SAr_2 chromophore. This possibility has not been investigated further.

^{51}V NMR Spectroscopy. Complexes **1**−**3** have well-resolved ^{51}V NMR spectra as one would anticipate for diamagnetic vanadium(V) complexes. However, in solution at least two species are present for each complex. As shown in Figure 3, complex **1** in CH_2Cl_2 solution gives four resonances at −378.0, −379.0, −381.0, and −383.6 ppm. These four resonances are most likely due to syn/anti and ligand exchange isomers as discussed below. Additionally, two minor resonances (due to **2**) occur −395 and −396 ppm in the spectrum of **1** in CH_2Cl_2 solution. Complex **2** gives two resonances of nearly equal intensity at −395.0 and −396.7 ppm.

The four downfield resonances in the solution of **1** may result from (a) bridge exchange and (b) syn/anti isomerization of the structurally characterized ethoxide-bridged dimer as shown in Scheme 1. The key step in these equilibria is the hydrolysis of one of the ethoxide bridges. Even with dry solvent (Aldrich 99.9% CH_2Cl_2; $H_2O \leq 0.02\%$), the water concentration is approximately 15 mM, which is several times the approximate concentration of the vanadium complexes in solution (1−2 mM). It is noted that **2** is synthesized using VO(O-*i*-Pr)$_3$ and using a freshly opened bottle of spectroscopic-grade acetonitrile. Under these conditions, the isopropoxide ligands do not compete with residual water in forming the bridges. Only when excess alkoxide is added, as in the case of **1**, is the alkoxide bridge complex formed. Thus, hydroxide is a competitive ligand in these systems.

In the absence of competing ethoxide ligands, the two resonances in **2** are due to syn/anti isomerization. Variation in the concentration of **2** (2.0−0.13 mM) has no effect on the ratio of the two peaks, indicating the two resonances are not due to a monomer−dimer equilibrium. Alternatively, linkage isomerism, in which the bridging and terminal ligands exchange, could explain these two peaks. We cannot distinguish these possibilities with the data currently available; however, we note that addition of excess ethanol to a CH_2Cl_2 solution of **2** yields complex **1** (by ^{51}V NMR), indicating that the hydroxide ligands are labile.

Complex **3** also shows two ^{51}V NMR resonances with the major peak at −416.1 ppm and a minor peak at −391.0 ppm; however, the chemical shift difference of $\Delta\delta = 25$ ppm indicates that these complexes are less closely related than the isomers of **1** ($\Delta\delta = 6$ ppm) and **2** ($\Delta\delta = 2$ ppm). The ratio of the two resonances in solutions of **3** is sensitive to the purity of the solvent with "dry" solvents giving less of the resonance at −391.0 ppm. Addition of water to a CH_2Cl_2 solution of **3** causes an increase in the resonance at −391.0 ppm consistent with hydrolysis of the equatorial mbp_2SO ligand in **3** to give a hydroxide-bridged dimer as shown in eq 3.

$$2VO(mbp_2SO)(Hmbp_2SO) + 2H_2O \rightarrow [VO(mbp_2SO)OH]_2 + 2H_2mbp_2SO \quad (3)$$

The line width of **3** (approximately 395 Hz) is significantly greater than that observed for **1** or **2**. This increased line width probably arises from a combination of quadrupolar broadening and chemical exchange effects. While all three complexes are six-coordinate, the three phenolate and sulfoxide equatorial donors of **3** should impose a greater electric field gradient at the vanadium nucleus as compared to the two phenolate, two alkoxide/hydroxide equatorial donors in **1** and **2**. Addition of water or alcohol to a solution of **3** gives rise to a similarly broad resonance at $\delta = -391$ ppm, indicating that a ligand exchange path exists that may contribute to the line width. Slight changes in the chemical shift of **3** upon addition of water may be due to solvent effects.

Electrochemistry. Cyclic voltammetry supports the presence of dimer structures in solution for the mbp_2S complexes, as shown in Figure 4. In CH_2Cl_2 solution, two cathodic waves are observed for **1** (−452 and −788 mV). Upon reversing the scan direction, two anodic waves (−364 and −668 mV) are observed that have approximately the same intensity as the cathodic signals, consistent with two quasi-reversible single-electron reductions of the V^V-V^V dimer ($E_{1/2} = -408$ and −728 mV). Complex **2** exhibits two cathodic waves (−424 and −723 mV) at about the same potential as observed for **1**; however, the corresponding anodic waves (−316 and −619 mV) are much less intense, consistent with irreversible electrochemistry under these conditions. The cyclic voltammograms of both **1** and **2** also have a relatively intense anodic wave at ≈ −180 mV. This is tentatively attributed to decomposition of the V^{IV} (or $V^{IV}-V^{IV}$) forms of **1** and **2**. As in the ^{51}V NMR experiments, addition of ethanol to CH_2Cl_2 solutions of **1** or **2** yields voltammograms (dashed voltammograms) for the pure ethanol bridged dimer. The differences in the peak separation ($\Delta E = 320$ mV for **1**) imply that the two redox processes are for a single dimeric species in which the redox centers are communicating, as one would expect for two vanadium(V) centers bridged by alkoxide or hydroxide bridges. These data give a comproportionation constant of $K_{com} \approx 10^5$. Only a single redox feature is observed in the cyclic voltammogram of **3**, as expected for a monomeric complex. The potential, $E_{1/2} = -502$ mV, suggests that the ML_2 coordination sphere of **3**, where L provides the harder sulfoxide oxygen donor, stabilizes the V^V oxidation state relative to **1** and **2**.

Oxygenation Studies. Several attempts have been made to oxygenate the coordinated sulfide of complexes **1** and **2** to form sulfoxide complexes such as **3**. In a two-phase system analogous to that used by Bolm and Bienewald for the catalytic oxygenation of sulfides (i.e., using CH_2Cl_2 as the solvent for **1** or **2**

Scheme 1

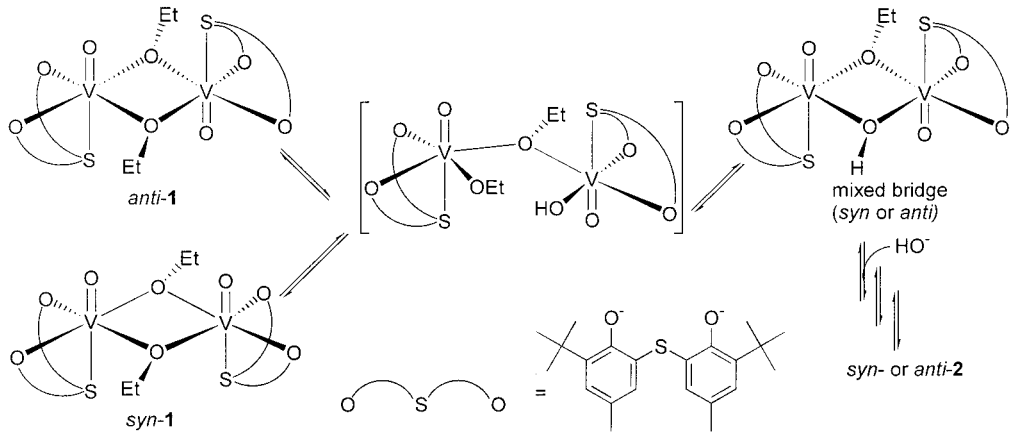

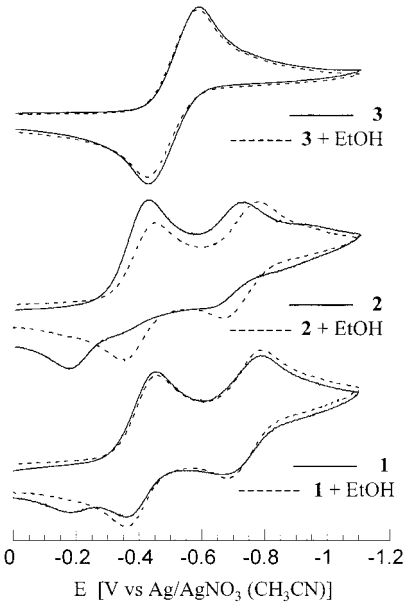

Figure 4. Cyclic voltammograms of **1**−**3** in CH_2Cl_2 solution.

and aqueous H_2O_2 (3%)),[4] ^{51}V NMR indicates only slow formation of **3**. During the course of the reaction, the purple organic phase becomes pale yellow and the ^{51}V NMR signal decreases, consistent with extraction of the vanadium into the aqueous peroxide layer. The colorless aqueous phase becomes red, consistent with the formation of an oxoperoxovanadium(V) solution.[36] The oxoperoxovanadium complexes can then oxygenate the sulfide to give H_2mbp_2SO. Upon catalytic decomposition of the excess peroxide, the sulfoxide ligand can re-ligate the vanadium to give **3**. In homogeneous systems using either *m*-CPBA or *t*-BuOOH (in hydrocarbon), slow decomposition of **1** or **2** gives multiple products that have not been characterized.

Conclusions

The sulfide-containing ligand $[mbp_2S]^{2-}$ coordinates facially to vanadium forming six-coordinate alkoxide- or hydroxide-bridged dimers (**1** and **2**, respectively). In these complexes, the sulfur donor is weakly coordinated trans to the oxo ligand. Vanadium-51 NMR indicates that structural isomers are present, and these have been assigned the syn and anti complexes of the dimers and mixed-bridge (alkoxide/hydroxide) species. Electrochemical studies indicate that the metal centers in **1** and **2** are strongly coupled ($K_{com} \approx 10^5$). Oxygenation of the sulfide-containing ligand yields the corresponding sulfoxide H_2mbp_2SO, which also coordinates to vanadium(V) to form six-coordinate complexes. However, the sulfoxide complexes have a 2:1 L:M stoichiometry in which one of the sulfoxide oxygens is coordinated trans to the oxo ligand and the other sulfoxide oxygen is coordinated in an equatorial site. This suggests that the sulfoxide oxygen of **3** is a better ligand than the sulfide sulfur of **1** or **2**. Under the conditions of this study, direct oxygenation of the coordinated sulfide in **1** and **2** has not been observed; however, the presence of excess hydrogen peroxide in solutions of **1** and **2** leads to the formation of **3** via oxoperoxovanadium(V) oxygenation of free H_2mbp_2S.

Acknowledgment. Funding for this work was provided by the National Science Foundation (CHE-9702873).

Supporting Information Available: Figure S1, UV−visible spectra of complexes **1**−**3** in CH_2Cl_2 (1 page). X-ray crystallographic files for **1**, **2**, and **3**, in CIF format, are available on the Internet only. This material is available free of charge via the Internet at http://pubs.acs.org.

IC9900253

(36) Butler, A.; Clague, M. J.; Meister, G. E. *Chem. Rev.* **1994**, *94*, 625−638.